Virtual Fragment Screening on GPCRs: a case study on Dopamine D3 and Histamine H4 Receptors

Márton Vass[a], Éva Schmidt[a], Ferenc Horti[a], György M. Keserű[b,*]

[a] Gedeon Richter Plc, H-1475, P.O.B. 27 Budapest, Hungary
[b] Research Centre for Natural Sciences of the Hungarian Academy of Sciences

* Corresponding author. Research Centre for Natural Sciences of the Hungarian Academy of Sciences, H-1525 P.O.B. 17, Budapest, Hungary. Tel: +36 1 438 1155; Fax: +36 1 438 1143; E-mail: keseru.gyorgy@ttk.mta.hu

Abstract

Prospective structure based virtual fragment screening methodologies on two GPCR targets namely the dopamine D3 and the histamine H4 receptors with a library of 12905 fragments were evaluated. Fragments were docked to the X-ray structure and the homology model of the D3 and H4 receptors, respectively. Representative receptor conformations for ensemble docking were obtained from molecular dynamics trajectories. *In vitro* confirmed hit rates ranged from 16% to 32%. Hits had high ligand efficiency (LE) values in the range of 0.31-0.74 and also acceptable lipophilic efficiency. The X-ray structure, the homology model and structural ensembles were all found suitable for docking based virtual screening of fragments against these GPCRs. However, there was little overlap among different hit sets and methodologies were thus complementary to each other.

1. Introduction

Fragment-based lead discovery (FBLD) has become a feasible alternative to traditional lead finding approaches in drug discovery employed both by industry and academic groups [1]. It has been demonstrated that starting from polar, low molecular weight – typically < 250 Da or less than 20 heavy atoms – compounds, leads and drugs with better physico-chemical properties can be achieved [2] even for difficult targets [3]. This view is supported by the increasing number of drug candidates recently entering clinical trials and one already approved drug originating from a fragment hit [4]. Since weakly binding fragments require sensitive, but typically lower throughput biophysical detection methodologies (such as SPR, NMR, XRD, MS), and also because fragments are usually optimized using structural information, there is an ongoing interest in virtual methodologies capable of predicting fragment binding and providing reliable binding modes for them. Molecular docking is an *in silico* tool aiming to predict the binding mode and binding free energy of druglike molecules. It has been shown that various docking programs have similar performance in pose prediction for fragments (especially for fragments of high ligand efficiency) and druglike molecules [5-7], since fragments usually exploit the specific interactions available at protein hot spots [8]. In virtual screening setups, where the objective is the ranking of fragments by binding free energy, the modest enrichment of actives [9,10] shall be improved using more accurate

binding free energy functions. One of these methods is the computationally intensive MM-PBSA rescoring method that was used to improve enrichments [11,12]. It has also been suggested that incorporating receptor flexibility in docking (not only in the rescoring phase) might be beneficial for virtual screening enrichments. Various protocols have been published taking into account different ranges of protein flexibility [13]. The simplest approach is the use soft potentials to account for small side-chain movements. Larger movements might be considered using side chain rotamer libraries. Docking into appropriately selected multiple protein conformations (ensemble docking) is a parallelizable and resource effective way of handling the flexibility of the entire protein. The most computationally intensive methods attempt the simultaneous conformational sampling of the receptor and the ligand, such as Schrödinger's Induced Fit Docking (IFD) [14] application, or running molecular dynamics (MD) simulation on each individual protein-fragment complex. Different receptor conformations for ensemble docking can be obtained from multiple crystal structures or NMR structures if such data is available. However, structural studies on membrane proteins, such as G protein-coupled receptors (GPCRs) typically represent great challenges. Despite recent progress in GPCR crystallization still only a small percentage of structures have been unveiled. In such a case homology modeling may be used to obtain an atomistic model of the receptor. Structurally diverse receptor models can be obtained using different GPCR template structures during homology modeling. Diverse conformations may also be sampled by MD simulation, Monte Carlo or low-mode conformational search starting from a single homology model [15,16]. De Graaf et al. used a homology model of the histamine H3 receptor and subsequent MD sampling to provide the conformations used for retrospective and prospective virtual fragment screening [17]. In the present study we performed prospective virtual fragment screening on the available dopamine D3 receptor crystal structure and a homology model of the histamine H4 receptor based on the recently solved histamine H1 receptor crystal structure. Snapshots from all-atom membrane-embedded MD simulations were also used for ensemble virtual screening of the same fragment library. Screening performance of the different protocols were compared analyzing hit rates and hit compounds obtained by docking to the single structure and the conformational ensembles.

2. Computational methods

2.1. Homology modeling and crystal structure preparation

The construction of the histamine H4 receptor homology model was described previously [18]. Briefly, the H4 amino acid sequence from the UniProt server (http://www.uniprot.org/) was aligned to the sequence of the template, the 3.1 Å resolution X-ray structure of the human histamine H1 receptor (PDB code: 3RZE) using Prime 3.0 [19]. The kink in helix TM4 was modeled based on the human β2-adrenergic receptor (PDB code: 2RH1). The JNJ7777120 ligand was first manually docked into the receptor, and then the 5 Å environment of the ligand was subjected to minimization with two H-bond constraints using MacroModel 9.9 [20]. JNJ7777120 was re-docked into the minimized structure using IFD [14,21] in the Schrödinger Suite 2011. Finally the whole structure was subjected to Impref restrained minimization in the Protein Preparation Wizard [22]. Chain A of the dopamine D3 crystal structure (PDB code: 3PBL) was subjected to the Protein Preparation Wizard workflow with default settings, that included assigning bond orders, adding hydrogens, creating disulfide bonds, optimization of the H-bond network and finally a restrained minimization of the complex.

2.2. Molecular dynamics simulations and ensemble preparation

The details of molecular dynamics simulations were described elsewhere [18]. Briefly, all-atom POPC membrane-embedded MD simulations were run starting from the homology model of the histamine H4 receptor JNJ7777120 complex and the crystal structure of the dopamine D3 receptor eticlopride complex using ff99SB force field for protein and GAFF force field for lipid and ligand atoms in the NAMD 2.7 [23] software. The systems were equilibrated with subsequent steps of i) 3200 steps minimization with restrained protein and ligand atoms ii) 3200 steps unrestrained minimization iii) heating in NVT ensemble to 310 K in 40 ps with restrained protein and ligand atoms iv) 1 ns MD simulation in $Np_z\gamma T$ ensemble with restrained protein and ligand atoms v) 1 ns MD simulation in $Np_z\gamma T$ ensemble with gradual removal of the restraints. 20 ns production runs in $Np_z\gamma T$ ensemble were conducted for both systems. Receptor conformations of the two trajectories were clustered using the average linkage method in the ptraj program from the AmberTools package [24] based on the RMSD of the amino acid residues that made up 90% cumulative occurrence in the 5 Å environment of the ligand. This method provided 28 representative conformations for the histamine H4 receptor and 27 representative conformations for the dopamine D3 receptor. All representatives were subjected to Impref restrained minimization in the Protein Preparation Wizard.

2.3. Single structure and ensemble docking methodologies

We collected 12905 fragment-like compounds from our in-house collection complying with an extended version of the Rule of Three: having an MW ≤ 300 Da, logP ≤ 3, number of H-bond donors and acceptors ≤ 3, number of rotatable bonds ≤ 6, PSA < 130 Å^2, containing 1-3 rings and no reactive functionalities (see property distributions and diversity assessment in the Supporting Information). The structures of these fragments were prepared using LigPrep 2.5 [25]. The dominant protonation and tautomeric state at pH 7.4 was calculated using Epik 2.2 [26]. Their logP was calculated using the ChemAxon cxcalc utility [27]. In the single structure investigation the 12905 fragments were docked into the binding site of the dopamine D3 X-ray structure and the histamine H4 homology model. Then in the ensemble docking approach the fragment set was docked into the binding sites of all representatives from the D3 and H4 MD trajectories. Glide 5.7 [28-31] software was used for docking. Grids for the initial homology model and crystal structure, as well as for the representatives from the MD trajectories were centered on the ligand centroids, and had dimensions of 14×14×14 Å for the inner box (which contains the ligand centroid during docking) and 44×44×44 Å for the outer box (which contains all ligand atoms during docking) to ensure that sampling of the binding mode was not biased by the grid size. Docking calculations were conducted using the single precision (SP) mode [5], with post-dock minimization performed for 15 poses. Only the top pose for each fragment by the Emodel scoring function was saved, which were ranked by the GlideScore scoring function for each individual receptor conformation. For single structure docking to the D3 X-ray structure and the H4 homology model, the top 50 compounds from the GlideScore ranked list were chosen for biological testing. In the ensemble docking approach mean ranks and their standard deviations calculated over the ensemble were used for evaluating each individual compound. Compounds having a mean rank lower than 500 were selected for biological testing. This cutoff gave a similar number of compounds to be tested as for the single structure case: 56 for the dopamine D3 receptor and 50 for the histamine H4 receptor.

3. Results and discussion

3.1. Receptor binding sites

While the histamine H1 and H4 receptors share 40% amino acid identity in the transmembrane region and they recognize the same endogenous ligand, there are substantial differences in their binding sites. For example Asn147$^{4.57}$ in H4 is equivalent to Trp158$^{4.56}$ in H1, Leu175$^{5.39}$ to Lys191$^{5.39}$, Glu182$^{5.46}$ to Asn198$^{5.46}$ and Gln347$^{7.42}$ to Gly457$^{7.42}$. Also, mutation of Asn147$^{4.57}$ and Glu182$^{5.46}$ showed significant alteration to JNJ7777120 inhibition constants [32]. Thus the initial homology model featured two specific H-bonds of JNJ7777120 to Asp94$^{3.32}$ and Glu182$^{5.46}$ as shown in Fig. 1A. In the course of the molecular dynamics simulation the H4 receptor binding site appears to be relatively rigid based on side chain χ_1 and χ_2 angles of the interacting residues (Fig. 2A). Met150$^{4.60}$ is quite flexible and Leu175$^{5.39}$ assumes two different rotamer states, but these variations don't alter the binding pattern of the ligand. However Glu182$^{5.46}$ also adopts two main rotamer states, which causes some variability in the ligand position within the binding site. The ionic interaction to Asp94$^{3.32}$ is mostly uninterrupted and surprisingly Gln347$^{7.42}$ also formed an H-bond with the carbonyl group of JNJ7777120 in some of the representative frames. The D3 receptor binding site is also quite rigid, only Cys114$^{3.36}$, Ser196$^{5.46}$ and Thr369$^{7.39}$ assume an alternative rotamer state featuring alternative H-bonds in a few representative structures (Fig. 2B). Interestingly, His349$^{6.55}$ was quite flexible, which seems to be in a tight H-bond network in the crystal structure. The ligand interaction pattern changed little; the highest RMSD from the crystal binding mode was 2.4 Å after superposition of the proteins, the ethylpyrrolidine part of eticlopride was able to move somewhat without losing the ionic interaction with Asp110$^{3.32}$ (shown in Fig. 1B).

3.2. Single structure and ensemble docking results

In the case of the H4 receptor the fragment library was docked to the homology model and to the 28 representative conformations collected from the molecular dynamics simulation, while for the D3 receptor docking has been carried out to the prepared X-ray structure and the 27 representative conformations from simulation. In both cases individual structural models provided a wide range of docking scores (GlideScore) but the single starting structure provided lower scores overall than the selected frames from MD. For example the docking scores of the top scoring fragments in each of the H4 frames ranged from -8.093 to -9.920 but it was -10.686 for the homology model. Similarly for the D3 receptor top scores ranged from -8.063 to -9.514 but it was -9.796 for the X-ray structure. Since binding sites appeared to be quite rigid during the MD simulation, these differences in the docking scores can be attributed to little variations in side chain geometries, indicating that specific interactions in the X-ray structure and homology model are in the optimal geometry with their respective ligands, while they loosen up during MD. Thus the distribution of the top scores indicate that X-ray structures and homology models have optimized protein-ligand interaction patterns while MD snapshots represent more diverse conformations, which in turn might be able to select more chemotypes than those optimized structures. For the single structures it was straightforward to select the top 50 fragments by GlideScore ranking for biological testing. For ensemble docking two different data fusion methods were considered. The rank-by-rank and rank-by-number consensus scoring schemes were investigated; the rank-by-vote method was shown to provide poorer results [33]. In the rank-by-rank scheme ligands are finally ranked by the mean of their rank numbers in each docking run to the representative structures. It was also investigated whether low standard deviation of ranks accompanies low mean ranks and we confirmed a strong correlation between average rank and its standard deviation for fragments

having mean rank lower than 500 (see Fig. 3). These fragments also fell in the top 1% of the ranked database in more than 3 representative frames both for the D3 and the H4 receptor. The correlation becomes less pronounced for higher mean ranks and eventually turns around for compounds ranked high by all MD frames. In the rank-by-number scheme ligands are finally ranked by the mean of their docking scores. It has been shown that using the mean of standardized Z-scores outperforms the average of the original scores; hence in this study the standardized GlideScores were evaluated. However, non-normal distribution of the GlideScores was observed for the fragment library and since there was two-thirds overlap between the top 50 selected by the rank-by-rank and rank-by-number schemes, the first one was finally used to select fragments for biological testing.

3.3. Pharmacological activities

In the case of the D3 receptor 50 fragments from the X-ray structure docking run and 56 fragments from the ensemble docking run were selected for biological testing. These lists had 14 compounds in common, thus altogether 92 fragments were tested for D3 binding affinity in 10 µM concentration. In the case of the H4 receptor 50 fragments from the initial homology model docking run and also 50 fragments from the ensemble docking run were selected for biological testing. These lists had 15 compounds in common, thus altogether 85 fragments were tested for H4 binding affinity in 10 µM concentration. The only 30% overlap between the different methods is not altogether surprising since the crystal structure and the homology model select compounds that bind to a specific receptor conformation while ensemble docking selects compounds that have reasonably good interaction patterns with multiple receptor conformations. It has also been shown that the overlap of hits picked up by different screening paradigms likewise might be very low [34]. In the case of D3 25 virtual hits provided higher than 20% inhibition in the biological assay, corresponding to a combined hit rate of 27% (hit rates are summarized in Table 1). Out of these 9 came from the crystal structure docking run (18% hit rate) and 18 from the ensemble docking run (32% hit rate) with only 2 overlapping compounds. Binding affinity was determined for the 8 best compounds exhibiting higher than 75% inhibition at 10 µM concentration (Table 2). K_i values were in the range of 0.17 to 2.8 µM. Besides binding affinity various ligand efficiency metrics are applied in fragment-based lead discovery in order to prioritize fragment hits. These metrics incorporate molecule size either in terms of molecular mass or heavy atom count and lipophilicity usually represented with the octanol-water partition coefficient logP. In this study ligand efficiency (LE = $-RT\ln K_i/N_{heavy}$) and lipophilic ligand efficiency (LELP = logP/LE) [2] were considered. Since the D3 ligands identified here are very tight binders, LE values much higher than the usually accepted lower limit of 0.3 were obtained. As they are also on the lower side of lipophilicity, LELP values mostly below 5 were found, compounds **2** and **4** being the most favorable. In the case of H4 somewhat fewer, 15 virtual hits provided higher than 20% inhibition in the biological assay, corresponding to a combined hit rate of 18%. Out of these 11 came from the homology model docking run (22% hit rate) and 8 from the ensemble docking run (16% hit rate) with 4 overlapping compounds. Five of them were unavailable in the compound collection in sufficient quantity for binding affinity measurement but K_i values were determined for the remaining 10 compounds (Table 3). These were in the range of 8.4 to 75 µM, an order of magnitude higher than the hits for the D3 receptor. The lower hit rate and the lower binding affinities indicate a difference in the chemical tractability of the two receptors. LE values of the H4 ligands were correspondingly not as high as for D3 but still above the 0.3 limit up to 0.45. Also, the H4 ligands were somewhat more lipophilic resulting in higher LELP values, though still below 10. Especially fragments **10** and **18** showed favorable LE and LELP values. Taken together, these fragments

would be suitable starting points for medicinal chemistry optimization; however, the scope of this study was to analyze the impact of different virtual fragment screening methodologies on hit finding. When hit-to-lead programs are initiated, novelty of the hits is also a crucial point. To assess this, substructure and similarity searches were conducted in the ChEMBL bioactivity database (https://www.ebi.ac.uk/chembldb/ accessed 21 January 2014). D3 hits were checked against all compounds with bioactivity data measured on the five dopamine receptors, while H4 hits against compounds with bioactivity data measured on the four histamine receptors. Exact substructure searches provided hits for **10** and **17**, and similarity searches revealed additional similar known structures (see Table 2 and Table 3). Compounds **2**, **4**, **8**, **15** and **18** proved to be truly novel ones, and others might also suggest potential unexplored growing vectors. Comparing the hit rates it can be seen that both X-ray structure and homology model were capable of providing useful hits in virtual screening, and in this particular case the homology model performed even better than the crystal structure. The superiority of the ensemble docking approach is not witnessed in this study. While for the D3 receptor the latter provided a substantially higher hit rate, the homology model performed best for the H4 receptor even though it was not preliminarily optimized in retrospective enrichment studies. Based on these results we conclude that both single structure and ensemble docking is useful for virtual fragment screening and seem to be complementary as the overlap between hit sets was low. Consequently a combined approach would maximize the outcome of hit finding efforts.

3.4. Binding modes

While no H-bond or pharmacophoric constraints were applied during docking the majority of the virtual hits in all four hit lists were basic amines forming ionic or H-bond interactions with the conserved Asp110$^{3.32}$ in D3 and the homologous Asp94$^{3.32}$ in H4 or the other acidic residue Glu182$^{5.46}$ also known to play an important role in the recognition of histamine in H4. In the case of the D3 receptor it was found that docked poses of the in vitro active fragments provided very similar binding modes in multiple representative receptor conformations obtained by molecular dynamics simulation. Also the fragment binding modes from the X-ray structure docking were pretty much similar to the ensemble binding modes further strengthening the probability of their biological significance [35]. For example the thiazolemethanamine **1** produced nine very similar binding modes in ensemble docking with the basic amine interacting with Asp110$^{3.32}$, the thiazole ring encased between Phe346$^{6.52}$ and Val111$^{3.33}$ and the chlorophenyl moiety facing His349$^{6.55}$ and Val350$^{6.56}$ with the chlorine substituent preferably pointing to the former, though in three poses pointing to the latter. The docked pose for the crystal structure is similar, though a bit shifted towards Asp110$^{3.32}$ and the chlorophenyl moiety rotated by 90 degrees and the chlorine pointing to Val350$^{6.56}$ (Fig. 4A). The tricyclic D3 fragment **2** is quite rigid and produced eleven very similar binding modes and also the binding mode in the crystal structure was almost identical. The basic amine group again forms an ionic H-bond to Asp110$^{3.32}$ and the aromatic ring almost overlaps with the chlorophenyl moiety of fragment **1**. In a few structures an H-bond between the fragment amide N-H and the hydroxyl group of Ser196$^{5.46}$ or the backbone carbonyl of Ser192$^{5.42}$ is percepted (Fig. 4B). In the case of the H4 receptor the picture was not as clear as for D3. There was substantially higher variability among docked poses in the ensemble approach and binding modes from docking to the homology model produced different results in more cases. The major cause for this was probably the different rotamer state of Glu182$^{5.46}$ in the homology model and in most of the representative frames from MD. Compound **9** for example produced a variety of binding modes probably because of its multiple H-bond donor sites, though it got good docking scores both in the homology model and in the representative

receptor conformations. Several similar poses were obtained for aminoquinoline **10**, in which the primary amine forms an ionic H-bond to Asp94$^{3.32}$, a cation-π interaction with Phe344$^{7.39}$ and the protonated quinoline nitrogen forms another ionic H-bond to Glu182$^{5.46}$. In the homology model the fragment is shifted towards the extracellular side of the pocket because of the greater distance between the two acidic sites, the quinoline ring is flipped and the anilinic N-H forms an additional H-bond to the phenolic OH of Tyr319$^{6.51}$ (Fig. 4C). Since this fragment was in the hit list from the homology model docking, the latter binding mode appears to be more feasible. For the tricyclic **18** seven similar poses were found in which the aliphatic amine group interacts with Asp94$^{3.32}$ and the carboaliphatic ring is encased between Tyr95$^{3.33}$, Met150$^{4.60}$ and Leu175$^{5.39}$. However, in four of these poses the protonated pyridine, while in three poses the anilinic N-H forms an H-bond with Glu182$^{5.46}$. The pose found in the homology model differs from both of them: it is rotated by 90° with the aliphatic amine again interacting with Asp94$^{3.32}$, the anilinic N-H with Glu182$^{5.46}$ the protonated pyridine with Gln347$^{7.42}$ and the carboaliphatic ring pointing towards the intracellular cavity of the binding site (Fig. 4D). Since this fragment was in the hit list from ensemble docking, the former binding mode appears to be more feasible. These findings underpin the superior hit rate for D3 and the inferior hit rate for H4 of the ensemble approach against the single structure hit rates. Also the higher binding affinities of D3 fragments correspond to the lower variability of their predicted binding modes [35].

4. Conclusions

In silico methods of fragment-based lead discovery have not yet been widely investigated for GPCR targets. In the present study we have evaluated prospective structure based virtual screening methodologies on two GPCR targets namely the dopamine D3 and the histamine H4 receptors and a fragment library of 12905 compounds. For both targets single structure and ensemble docking screens were performed. For the D3 receptor the X-ray structure with eticlopride was available for the single structure screen, while a previously constructed H1 receptor based homology model of H4 was utilized. Representative receptor conformations for ensemble docking were generated by molecular dynamics simulations. Around 50 virtual hits from both methodologies for both receptors were measured *in vitro* and with a greater than 20% inhibition at 10 μM criterion confirmed hit rates ranged from 16% to 32%. The reported hits provided high LE and low LELP values and are suitable starting points for hit-to-lead optimization. Analysis of the obtained binding modes provided insight to the variation in hit rates of the different methodologies. It was found that the X-ray structure, the homology model and structural ensembles are all suitable for docking based virtual screening of fragments against these GPCRs. However, there was little overlap among their hit sets and were thus complementary to each other. Combined approaches should provide valuable starting points for fragment-based lead discovery for other GPCRs as well if an X-ray structure or a good quality homology model is available.

5. Experimental

5.1 Human recombinant D3 binding assay

Cell cultures (CHO-K1) expressing human D3 receptors (purchased from HD Euroscreen Fast, Belgium) were homogenized in buffer solution (composition: 15 mM Tris, 2 mM MgCl$_2$, 0,3 mM EDTA, 1 mM EGTA, pH=7.4 at 25°C) in 4x v/w with a Dounce tissue grinder and centrifuged at 40000 g at 4°C for 25 min. The supernatant was removed and the pellet was resuspended in 4x v/w buffer and recentrifuged. This process was repeated twice

more and the pellet was resuspended in buffer (composition: 75 mM Tris, 12,5 mM MgCl$_2$, 0,3 mM EDTA, 1 mM EGTA, 250 mM Sucrose, pH=7.4 at 25°C) at a volume of 12,5 mL/g original weight. The preparations were then aliquoted and stored at -70°C.

The aliquoted membrane was thawed and washed once in binding buffer containing 50 mM Tris-HCl; 5 mM MgCl$_2$, 5 mM KCl; 1 mM CaCl$_2$, 120 mM NaCl, 1 mM EDTA. In the same buffer 3,3 µg protein/assay was incubated with 2 nM [^{3}H]raclopride in the presence or absence of test compound (to determine the binding inhibition of the test compound or the total binding, respectively) for 120 minutes at 25°C at a volume of 250 µL in 96 Deep Well plate. Non-specific binding was determined in the presence of 10 µM haloperidol. After incubation, samples were filtered over UniFilter$^®$ GF/B^{TM} using PerkinElmer Harvester and washed with 4x1 mL ice-cold binding buffer. The plate was dried at 40°C for an hour and 40 µL Microscint scintillation cocktail (PerkinElmer) was added to each well. The radioactivity was determined in MicroBeta 2450 microplate counter (PerkinElmer).

SEM was lower than 15% for single concentration measurements and lower than 7% for the hits. The ligand displacement experiments were repeated at least two times. The specific radioligand binding is defined as the difference between total binding and the non-specific binding determined in the presence of an excess amount of haloperidol. IC$_{50}$ values (i.e. concentration of compound giving 50% inhibition of specific binding) were determined from concentration-displacement curves by sigmoidal fitting. The inhibition constants (K$_i$) were calculated using the Cheng-Prusoff equation: K$_i$ = IC$_{50}$/[1+(L/K$_D$)], where [L] is the free radioligand concentration and K$_D$ the affinity of the labeled ligand for receptor. K$_D$ was determined from the Scatchard plot. GraFit 6.0 (Erithracus Software, Horley, UK) software was used for curve fittings.

5.2 Human recombinant H4 binding assay

Membranes from CHO-K1 cells expressing human histamine H4 receptors were purchased from PerkinElmer Life and Analytical Sciences (Cat. No. ES-393-M400UA). Frozen membrane aliquots were thawed at room temperature and diluted to 200-fold (15 µg protein/500µL diluted membrane/well) with binding buffer (50 mM TRIS-HCl pH 7.4, 5 mM EDTA).

The assay was performed according to the PerkinElmer assay protocol for human H4 receptor: 500 µL diluted membrane suspension (15 µg protein/assay) was incubated with [^{3}H]histamine as radioligand . Final reaction volume was 550 µL and final radioligand concentration was 4-7 nM. 10 µM histamine was used for determination of non-specific binding. The samples were incubated at 27°C for 30 min and binding was terminated by vacuum filtration through Whatman GF/B glass fiber filters, pre-soaked in 0.5 % PEI. The filters were washed 3-times with 4 mL ice cold binding buffer. Filters were transferred to vials, 4 mL Optiphase HiSafe scintillation cocktail (PerkinElmer) was added and radioactivity was determined by Packard TriCarb 2900 TR (PerkinElmer) liquid scintillation counter.

SEM was lower than 15% for single concentration measurements and lower than 7% for the hits. The ligand displacement by the compounds was determined using a minimum of six concentrations in duplicate or triplicate, and experiments were repeated at least two times. The specific radioligand binding is defined as the difference between total binding and the non-specific binding determined in the presence of an excess of unlabelled ligand. IC$_{50}$ values (i.e. concentration of compound giving 50% inhibition of specific binding) were determined from concentration-displacement curves by sigmoidal fitting using Prism Software 4.0 (GraphPad, San Diego, CA, U.S.A.). K$_i$ values (i.e. inhibition constants) were calculated using the Cheng-Prusoff equation: K$_i$ = IC$_{50}$/[1+(L/K$_D$)], where [L] is the free radioligand

concentration and K_D the affinity of the labelled ligand for receptor. K_D was determined from the Scatchard plot.

Supporting information

Contains property distributions and diversity assessment of the fragment collection and dose-response curves of the exemplified fragment hits.

Acknowledgements

References

[1]   M. Baker, Fragment-based lead discovery grows up, Nat. Rev. Drug. Discov. 12 (2013) 5-7.

[2]   G.G. Ferenczy, G.M. Keserű, How are fragments optimized? A retrospective analysis of 145 fragment optimizations, J. Med. Chem. 56 (2013) 2478-2486.

[3]   A. Stamford, C. Strickland, Inhibitors of BACE for treating Alzheimer's disease: a fragment-based drug discovery story, Curr. Opin. Chem. Biol. 17 (2013) 320-328.

[4]   J. Tsai, J.T. Lee, W. Wang, J. Zhang, H. Cho, S. Mamo, R. Bremer, S. Gillette, J. Kong, N.K. Haass, K. Sproesser, L. Li, K.S. Smalley, D. Fong, Y.L. Zhu, A. Marimuthu, H. Nguyen, B. Lam, J. Liu, I. Cheung, J. Rice, Y. Suzuki, C. Luu, C. Settachatgul, R. Shellooe, J. Cantwell, S.H. Kim, J. Schlessinger, K.Y. Zhang, B.L. West, B. Powell, G. Habets, C. Zhang, P.N. Ibrahim, P. Hirth, D.R. Artis, M. Herlyn and G. Bollag, Discovery of a selective inhibitor of oncogenic B-Raf kinase with potent antimelanoma activity, Proc. Natl. Acad. Sci. U.S.A. 105 (2008) 3041-3046.

[5]   M. Sándor, R. Kiss, G.M. Keserű, Virtual fragment docking by Glide: a validation study on 190 protein-fragment complexes, J. Chem. Inf. Model. 50 (2010) 1165-1172.

[6]   M.L. Verdonk, I. Giangreco, R.J. Hall, O. Korb, P.N. Mortenson, C.W. Murray, Docking performance of fragments and druglike compounds, J. Med. Chem. 54 (2011) 5422-5431.

[7]   M. Vass, G.M. Keserű, Fragments to link. A multiple docking strategy for second site binders, Med. Chem. Commun. 4 (2013) 510-514.

[8]   G.G. Ferenczy, G.M. Keserű, Thermodynamics of fragment binding, J. Chem. Inf. Model. 52 (2012) 1039-1045.

[9]   S. Kawatkar, H. Wang, R. Czerminski, D. Joseph-McCarthy, Virtual fragment screening: an exploration of various docking and scoring protocols for fragments using Glide, J. Comput. Aided. Mol. Des. 23 (2009) 527-539.

[10]   A. Kumar, K.Y. Zhang, Computational fragment-based screening using RosettaLigand: the SAMPL3 challenge, J. Comput. Aided. Mol. Des. 26 (2012) 603-616.

[11]   S. Kawatkar, D. Moustakas, M. Miller, D. Joseph-McCarthy, Virtual fragment screening: exploration of MM-PBSA re-scoring, J. Comput. Aided. Mol. Des. 26 (2012) 921-934.

[12]   T. Zhu, H. Lee, H. Lei, C. Jones, K. Patel, M.E. Johnson, K.E. Hevener, Fragment-Based Drug Discovery Using a Multidomain, Parallel MD-MM/PBSA Screening Protocol, J. Chem. Inf. Model. 53 (2013) 560-572.

[13]   C. B-Rao, J. Subramanian, S.D. Sharma, Managing protein flexibility in docking and its applications, Drug. Discov. Today. 14 (2009) 394-400.

[14]   W. Sherman, T. Day, M.P. Jacobson, R.A. Friesner, R. Farid, Novel procedure for modeling ligand/receptor induced fit effects. J. Med. Chem. 49 (2006) 534-553.

[15]   D.J. Osguthorpe, W. Sherman, A.T. Hagler, Exploring protein flexibility: incorporating structural ensembles from crystal structures and simulation into virtual screening protocols, J. Phys. Chem. B. 116 (2012) 6952-6959.

[16]   C.N. Cavasotto, J.A. Kovacs, R.A. Abagyan, Representing receptor flexibility in ligand docking through relevant normal modes, J. Am. Chem. Soc. 127 (2005) 9632-9640.

[17]   F. Sirci, E.P. Istyastono, H.F. Vischer, A.J. Kooistra, S. Nijmeijer, M. Kuijer, M. Wijtmans, R. Mannhold, R. Leurs, I.J. de Esch, C. de Graaf, Virtual fragment screening: discovery of histamine H3 receptor ligands using ligand-based and protein-based molecular fingerprints. J. Chem. Inf. Model. 52 (2012) 3308-3324.

[18]   A. Tarcsay, G. Paragi, M. Vass, B. Jójárt, F. Bogár, G.M. Keserű, The impact of molecular dynamics sampling on the performance of virtual screening against GPCRs. J. Chem. Inf. Model. 53 (2013) 2990-2999.

[19]   Prime, version 3.0, Schrödinger, LLC, New York, NY, 2012.

[20]   MacroModel, version 9.9, Schrödinger, LLC, New York, NY, 2012.

[21]   Schrödinger Suite 2011 Induced Fit Docking protocol; Glide version 5.7, Schrödinger, LLC, New York, NY, 2011; Prime version 3.0, Schrödinger, LLC, New York, NY, 2011.

[22]   Schrödinger Suite 2011 Schrödinger Suite; Epik version 2.2, Schrödinger, LLC, New York, NY, 2011; Impact version 5.7, Schrödinger, LLC, New York, NY, 2011; Prime version 2.3, Schrödinger, LLC, New York, NY, 2011.

[23]   J.C. Phillips, R. Braun, W. Wang, J. Gumbart, E. Tajkhorshid, E. Villa, C. Chipot, R.D. Skeel, L. Kalé, K. Schulten, Scalable molecular dynamics with NAMD, J. Comput. Chem. 26 (2005) 1781-1802.

[24]   D.A. Case, T.E. Cheatham, T. Darden, H. Gohlke, R. Luo, K.M. Merz, A. Onufriev, C. Simmerling, B. Wang, R.J. Woods, The Amber biomolecular simulation programs, J. Comput. Chem. 26 (2005) 1668-1688.

[25]   LigPrep, version 2.5, Schrödinger, LLC, New York, NY, 2011.

[26]   Epik, version 2.2, Schrödinger, LLC, New York, NY, 2011.

[27]   Calculator, version 5.10.2, © 1998–2012 ChemAxon Ltd.

[28]   Glide, version 5.7, Schrödinger, LLC, New York, NY, 2011.

[29]   R.A. Friesner, J.L. Banks, R.B. Murphy, T.A. Halgren, J.J. Klicic, D.T. Mainz, M.P. Repasky, E.H. Knoll, D.E. Shaw, M. Shelley, J.K. Perry, P. Francis, P.S. Shenkin, Glide: A New Approach for Rapid, Accurate Docking and Scoring. 1. Method and Assessment of Docking Accuracy, J. Med. Chem. 47 (2004) 1739-1749.

[30]   T.A. Halgren, R.B. Murphy, R.A. Friesner, H.S. Beard, L.L. Frye, W.T. Pollard, J.L. Banks, Glide: A New Approach for Rapid, Accurate Docking and Scoring. 2. Enrichment Factors in Database Screening, J. Med. Chem. 47 (2004) 1750–1759.

[31]   R.A. Friesner, R.B. Murphy, M.P. Repasky, L.L. Frye, J.R. Greenwood, T.A. Halgren, P.C. Sanschagrin, D.T. Mainz, Extra Precision Glide: Docking and Scoring Incorporating a Model of Hydrophobic Enclosure for Protein-Ligand Complexes, J. Med. Chem. 49 (2006) 6177–6196.

[32]   H.D. Lim, C. de Graaf, W. Jiang, P. Sadek, P.M. McGovern, E.P. Istyastono, R.A. Bakker, I.J. de Esch, R.L. Thurmond, R. Leurs, Molecular determinants of ligand binding to H4R species variants, Mol. Pharmacol. 77 (2010) 734-743.

[33]   R. Wang, S. Wang, How does consensus scoring work for virtual library screening? An idealized computer experiment, J. Chem. Inf. Comput. Sci. 41 (2001) 1422-1426.

[34]   J. Wielens, S.J. Headey, D.I. Rhodes, R.J. Mulder, O. Dolezal, J.J. Deadman, J. Newman, D.K. Chalmers, M.W. Parker, T.S. Peat, M.J. Scanlon, Parallel screening of low

molecular weight fragment libraries: do differences in methodology affect hit identification? J. Biomol. Screen. 18 (2013) 147-159.

[35]   M. Orita, K. Ohno, M. Warizaya, Y. Amano, T. Niimi, Lead generation and examples opinion regarding how to follow up hits. Methods Enzymol. 493 (2011) 383-419.

Keywords

fragment screening, fragment docking, virtual screening, ensemble docking, G protein-coupled receptors, dopamine D3 receptor, histamine H4 receptor

Highlights

- A library of 12905 fragments was virtually screened by docking against two GPCRs.
- The D3 X-ray structure, a H4 homology model and representative frames for both receptors from MD were used.
- Single structure and ensemble docking hit rates ranged from 16% to 32%.
- Overlap between hit sets was low, methodologies were complementary.
- Structural background of hit rates was analyzed.

Abbreviations: GPCR: G protein-coupled receptor; FBLD: fragment-based lead discovery; LE: ligand efficiency; LELP: ligand-efficiency-dependent lipophilicity; MD: molecular dynamics; IFD: induced fit docking; POPC: 1-palmitoyl-2-oleoylphosphatidylcholine; RMSD: root-mean-square deviation; SP: single precision.

Graphical abstract
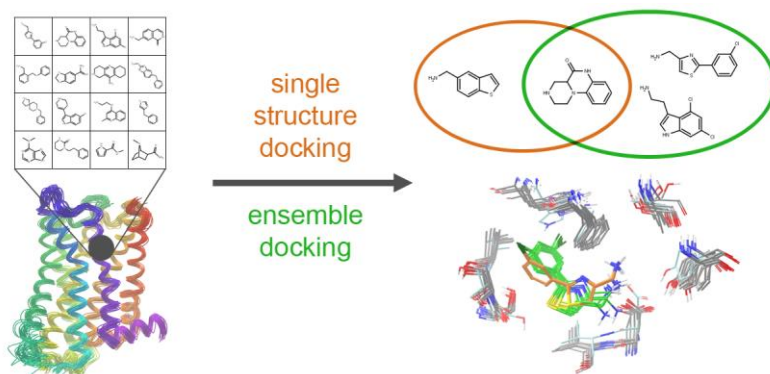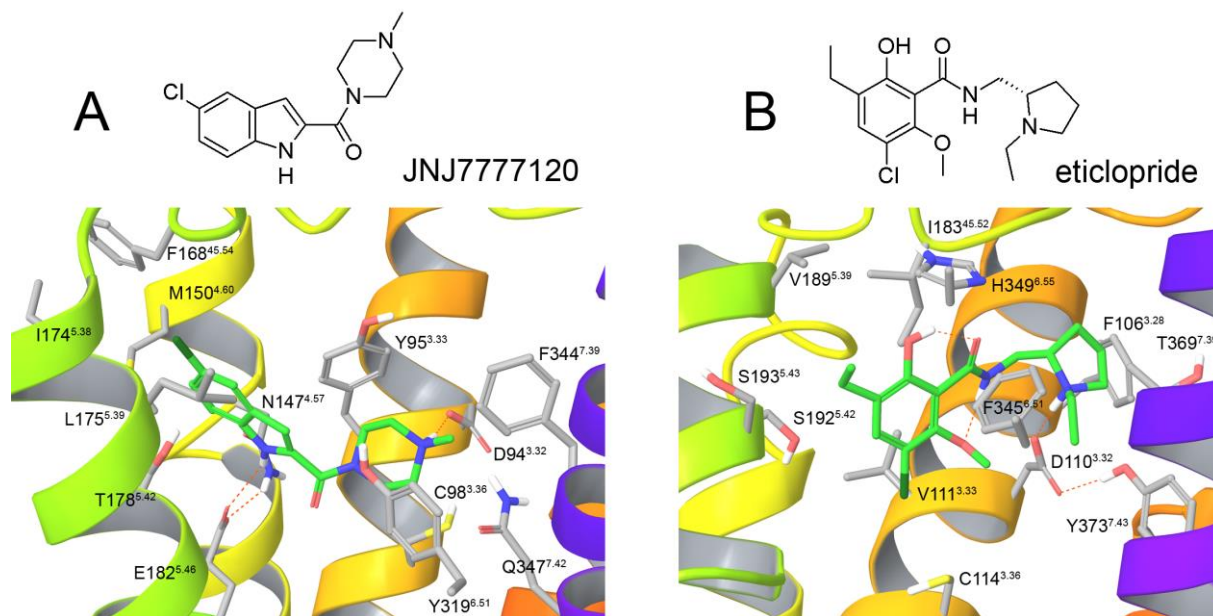
Fig. 1. Ligand structures and binding pockets of the initial receptor structures. A) Homology model of the human histamine H4 receptor in complex with JNJ7777120; B) X-ray structure of the human dopamine D3 receptor in complex with eticlopride. Receptors are represented as ribbons (helix 6 omitted for clarity) with interacting amino acids and ligands in grey and green skeletons, respectively and H-bonds in orange dash line.
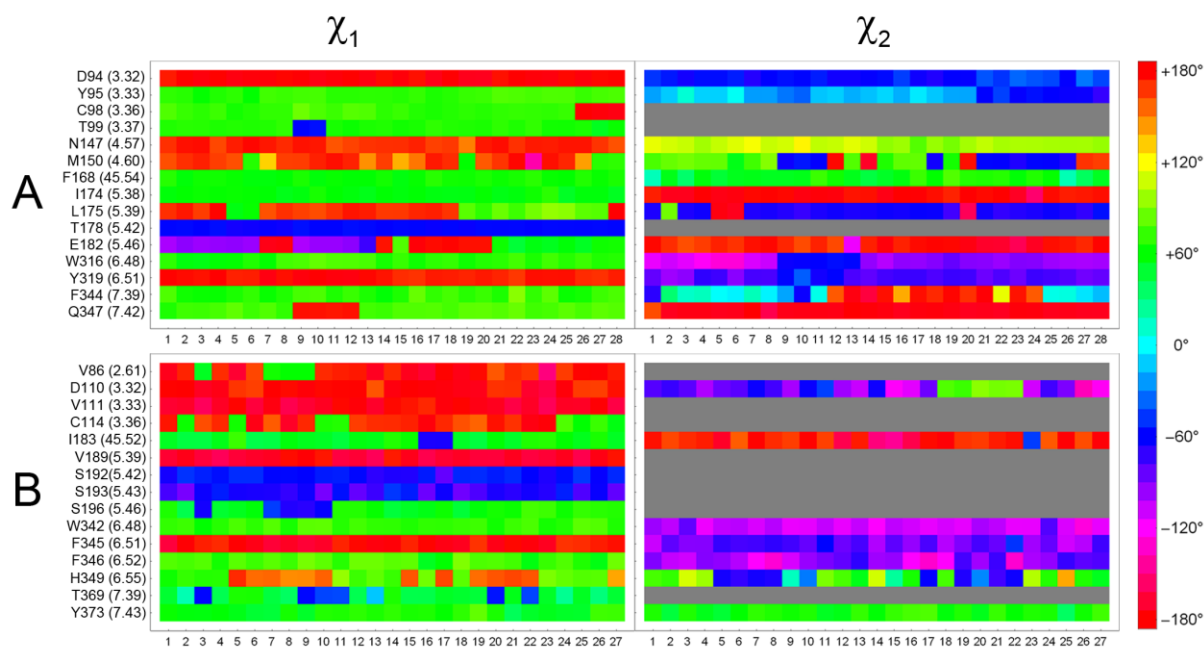
Fig. 2. Conformational variability of the binding sites: χ_1 and χ_2 side chain angles of binding site amino acids for each representative molecular dynamics frame in A) the H4 receptor and B) the D3 receptor. Angles are color coded according to the legend.
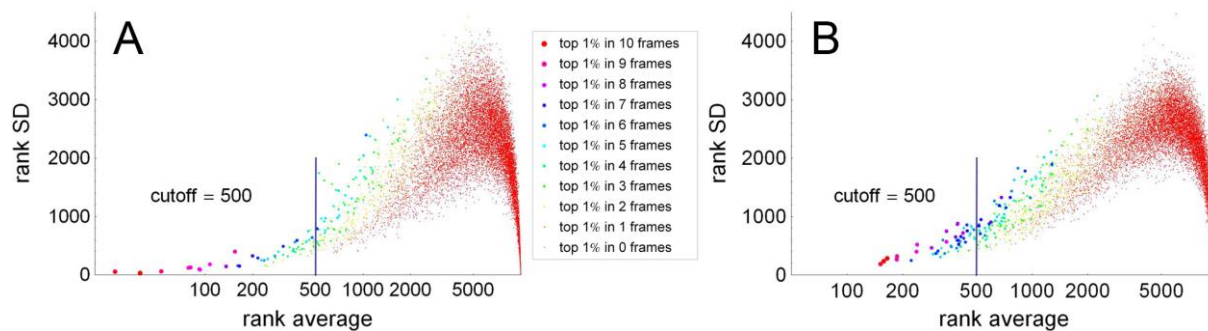
Fig. 3. Log-linear plot of fragment rank averages and standard deviations of ranks in the ensemble docking approach for A) the D3 receptor and B) for the H4 receptor. Rank standard deviation is plotted against rank average calculated from the ranks obtained in the representative receptor structures for the 12905 fragments. Markers are size and color coded by the number of receptor frames in which the fragment fell within the top 1% of the ranked library.
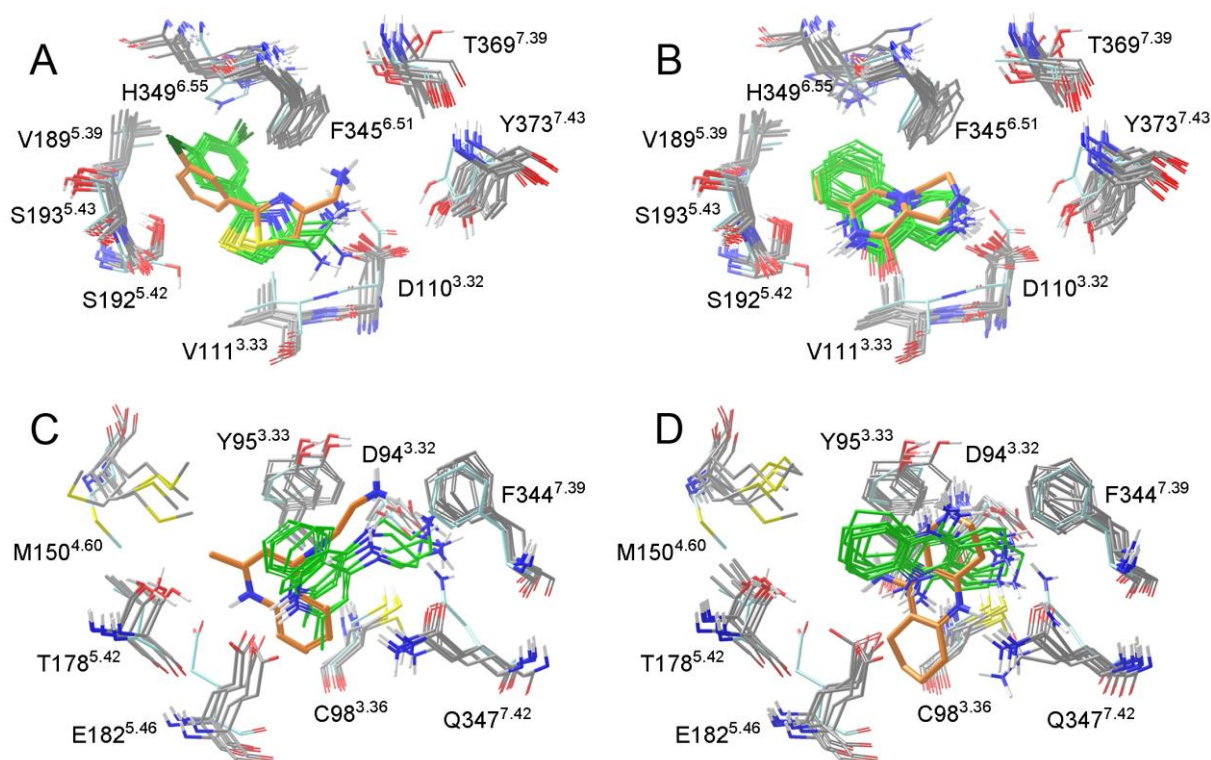
Fig. 4. Interaction modes of selected fragment hits obtained by single structure and ensemble docking. A) **1** in the D3 binding pocket; B) **2** in the D3 binding pocket; C) **10** in the H4 binding pocket; D) **18** in the H4 binding pocket. Selected interacting amino acids of the crystal structure and the homology model are shown in light blue skeleton, those of the representative MD frames in grey, single structure docked fragment poses in orange and ensemble docked poses in green skeletons. In A) and B) Phe346$^{6.52}$, Val350$^{6.56}$ and Ser196$^{5.46}$ are omitted for clarity. In C) and D) Tyr319$^{6.51}$ and Leu175$^{5.39}$ are omitted for clarity.

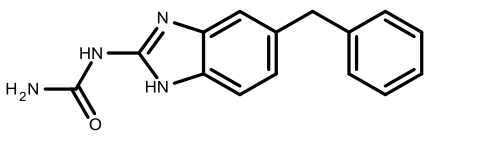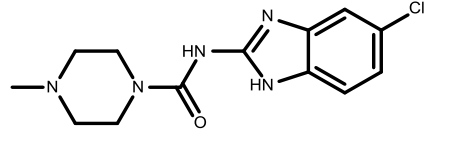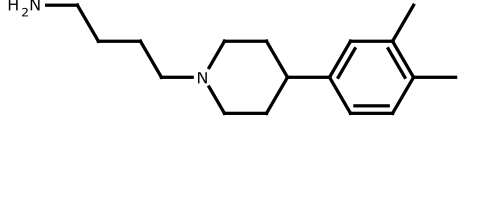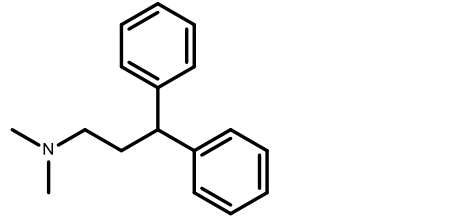|	D3	H4
combined hit rate	25/92 (27%)	15/85 (18%)
single structure hit rate	9/50 (18%)	11/50 (22%)
ensemble docking hit rate	18/56 (32%)	8/50 (16%)
overlap between hit sets	2/25 (8%)	4/15 (27%)
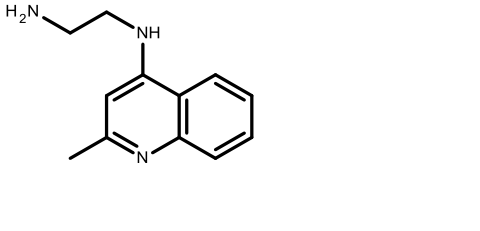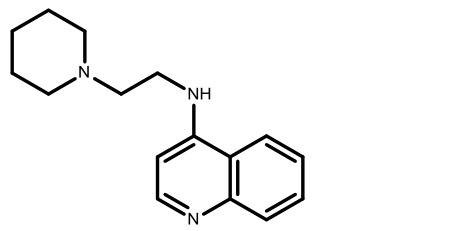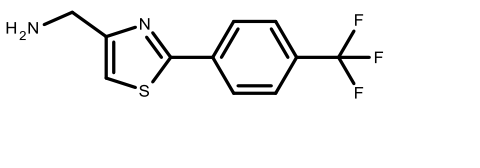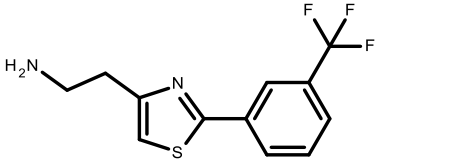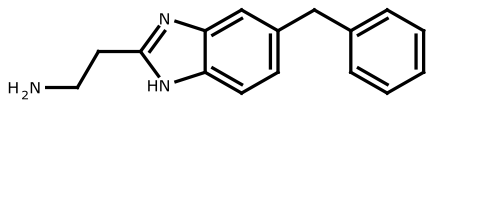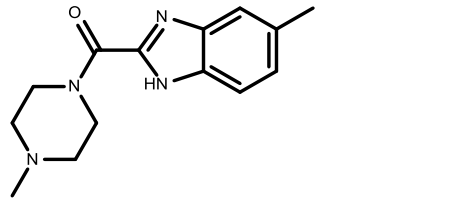
Table 1. Hit rate statistics for the two receptors considered in this study. Hits are defined as showing higher than 20% inhibition in the D3 and H4 radioligand binding assays.

cpd	Structure	hD3 K_i / μM	LE	LELP	XRD	MD	Closest known $D_{1-5}R$ ligand
1		0.17	0.66	3.7		+	
2		0.50	0.57	1.2	+	+	
3		0.59	0.61	4.4		+	
4		1.1	0.63	0.7		+	
5		1.1	0.74	2.7	+		

cpd	Structure						Closest known ligand
6		1.6	0.66	4.2		+	
7		2.8	0.47	5.6	+		
8		2.8	0.40	4.2		+	

Table 2. Experimental binding affinities of selected fragment hits of the D3 receptor and their LE and LELP values. The origin of the hit is indicated in the XRD and MD columns with + meaning the fragment was a virtual hit in the crystal structure docking or in the ensemble docking, respectively. Closest structural analogs from ChEMBL with measured binding affinity or functional activity against any of the five dopamine receptors are also indicated.

cpd	Structure	hH4 K_i / μM	LE	LELP	HM	MD	Closest known H$_{1-4}$R ligand
9		8.4	0.35	6.4	+	+	

10		12.6	0.45	2.1	+		
11		14.3	0.39	7.1	+		
12		20.6	0.34	8.3	+		
13		21.9	0.32	9.3	+		
14		32.0	0.31	7.4	+		
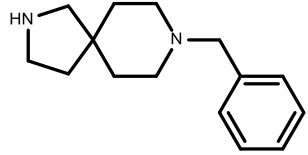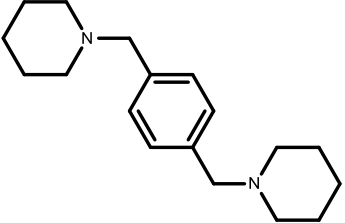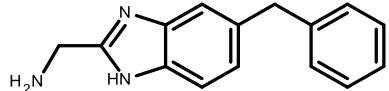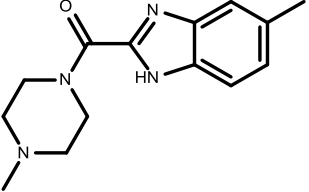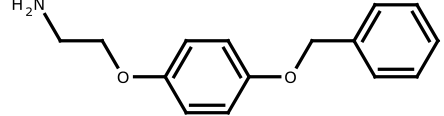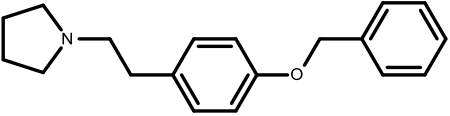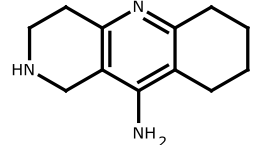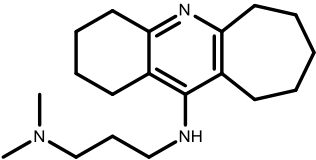
15		32.9	0.36	5.4	+	+	
16		58.4	0.32	8.0	+	+	
17		58.7	0.32	8.1	+		
18		75.1	0.37	2.3		+	

Table 3. Experimental binding affinities of selected fragment hits of the H4 receptor and their LE and LELP values. The origin of the hit is indicated in the HM and MD columns with + meaning the fragment was a virtual hit in the homology model docking or in the ensemble docking, respectively. Closest structural analogs from ChEMBL with measured binding affinity or functional activity against any of the four histamine receptors are also indicated.